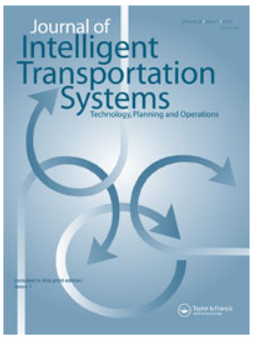

Taylor & Francis
Taylor & Francis Group

Journal of Intelligent Transportation Systems
Technology, Planning, and Operations

ISSN: 1547-2450 (Print) 1547-2442 (Online) Journal homepage: www.tandfonline.com/journals/gits20

A study of the environmental impacts of intelligent automated vehicle control at intersections via V2V and V2I communications

Luís Conde Bento, Ricardo Parafita, Hesham A. Rakha & Urbano J. Nunes

To cite this article: Luís Conde Bento, Ricardo Parafita, Hesham A. Rakha & Urbano J. Nunes (2019) A study of the environmental impacts of intelligent automated vehicle control at intersections via V2V and V2I communications, Journal of Intelligent Transportation Systems, 23:1, 41-59, DOI: 10.1080/15472450.2018.1501272

To link to this article: https://doi.org/10.1080/15472450.2018.1501272

JOURNAL OF INTELLIGENT TRANSPORTATION SYSTEMS
2019, VOL. 23, NO. 1, 41–59
https://doi.org/10.1080/15472450.2018.1501272

A study of the environmental impacts of intelligent automated vehicle control at intersections via V2V and V2I communications

Luís Conde Bento[a,b], Ricardo Parafita[a], Hesham A. Rakha[c], and Urbano J. Nunes[a]

[a]ISR-Institute of Systems and Robotics, Electrical and Computer Eng. Department, University of Coimbra, Coimbra, Portugal; [b]ESTG, Polytechnic Institute of Leiria, Leiria, Portugal; [c]Charles E. Via, Jr. Department of Civil and Environmental Engineering at Virginia Tech and the Virginia Tech Transportation Institute, Blacksburg, VA, USA

ABSTRACT

This article presents a novel intersection traffic management system for automated vehicles and quantifies its impact on fuel consumption and greenhouse gas emissions of CO_2 relative to traditional traffic signal and roundabout intersection control. The developed intelligent traffic management (ITM) techniques, which are based on a spatiotemporal reservation scheme, ensure that vehicles proceed through the intersection without colliding with other vehicles while at the same time reducing the intersection delay and environmental impacts. Specifically, the spatiotemporal reservation scheme provides each vehicle a collision-free path that is decomposed into a speed profile along with navigational instructions. The integration of the developed microscopic traffic simulator with instantaneous emission model, provides improved assessments of the environmental impact of traffic control strategies at intersections. The simulator architecture integrates several ITM algorithms, vehicle sensors, V2V/V2I communications, and emission and fuel consumption models. Each vehicle is modeled by an agent and each agent provides information depending on the specific vehicle sensors. The ITM system is supported by V2V and V2I communications, allowing the exchange of information among vehicles and infrastructure. The data include the estimated vehicle position and speed. Compared with traditional traffic management techniques, the simulation results prove that the proposed ITM system reduces CO_2 emissions significantly. The research also shows that these reductions are more significant when the traffic flow increases.

ARTICLE HISTORY
Received 22 October 2014
Revised 17 June 2018
Accepted 17 June 2018

KEYWORDS
Intelligent traffic management; vehicle fuel consumption; vehicle greenhouse gas emissions; vehicle simulation

Introduction

Global warming is a very serious problem, which is worsening with the growth of traffic congestion, due to the increasing number of vehicles on roads. New strategies, namely automated driving and connected vehicles, are required to cope with the increased traffic congestion, fuel consumption, and CO_2 emissions (Milakis, Arem, & Wee, 2017).

Environmental evaluation using macroscopic traffic simulators has been reported (Sharma & Mishra, 2013). However, macroscopic traffic simulators are not appropriate for modeling vehicle accelerations and capturing their impact on the environment, as is the case with traffic signals or traffic jams, where stop-and-go driving occurs (Yao & Yuanyuan, 2013). Alternatively, microscopic traffic simulators can reproduce both traffic jams and vehicle accelerations most common at intersections (Driel & Arem, 2010; Olia, Abdelgawad, Abdulhai, & Razavi, 2016).

Vehicle collisions at intersections account for a large percentage of overall traffic accidents, a significant portion of which are fatal. Much work has been done in the field of crossroad intersections (CI) (Dresner & Stone, 2008; Ferreira & Orey, 2012; Minjie, Xu, Hongyu, Linghe, & Minglu, 2009; Qiu, Guoyuan, Boriboonsomsin, & Barth, 2012; Shan, Sadek, & Yunjie, 2012). Dresner and Stone (2008) and Minjie et al. (2009) focused their work on intelligent traffic management (ITM) at intersections using microscopic models. Dresner and Stone (2008) developed an ITM based on a time slot reservation scheme for a crossroad intersection. Minjie et al. (2009) minimized the average intersection delay and the traffic collisions by distributing passing permissions among vehicles. Although there are significant number of roundabout intersections (RI) nowadays, not much work has been done to automatically regulate traffic at such intersections (Zohdy & Rakha, 2016). Most of

CONTACT Luís Conde Bento conde@isr.uc.pt ISR-Institute of Systems and Robotics, Electrical and Computer Eng. Department, University of Coimbra, Coimbra, Portugal.
Color versions of one or more of the figures in the article can be found online at www.tandfonline.com/gits

the research has been made on the traffic management or on CO_2 emissions modeling, with few efforts addressing the CO_2 emissions in the development of traffic control strategies at a microscopic level.

There is a wide range of traffic simulators available (Zohdy & Rakha, 2013), nevertheless, all traffic simulators lack key ingredients needed for algorithmic development related to automated vehicles, namely being proprietary and a lack of detailed sensor simulation. The simulation of sensors and their noise characteristics are possible using simulators from the area of robotics (e.g., Gazebo and USARSim), but these simulators lack both the vehicular communications and vehicle emission models. Vehicular communications are composed of V2V and V2I communications.

In this article, we use vehicle-to-vehicle (V2V) and vehicle-to-infrastructure (V2I) communications and accurate positioning systems, as important tools to assist ITM to regulate traffic and reduce CO_2 emissions. A spatiotemporal matrix reservation scheme provides a vehicle speed profile. The simulation results reported in this article were obtained with our developed microscopic simulator ISR-TRAFSIM (ISR Traffic Simulator) (Bento, Parafita, & Nunes, 2012a) [available at http://home.isr.uc.pt/~conde/isr-trafsim/]. A new module for instantaneous emissions computation, herein, detailed was added to the ISR-TRAFSIM.

The following algorithms have been implemented and extensive comparative tests have been performed:

- STLS – Standard Traffic Light System;
- ITMD – Intelligent Traffic Management Deactivated;
- CIITM – Crossroad Intersection Intelligent Traffic Management;
- WMITM – Waiting Method Intelligent Traffic Management;
- EMITM – Early Method Intelligent Traffic Management.

The research described in this article makes the following contributions to existing literature. First, the study uses absolute positioning systems, namely a simulated Global Navigation Satellite System (GNSS), to estimate the vehicles' pose. Second, a detailed fuel consumption and emissions model, from low level to high level, was used to evaluate the environmental benefits of the reservation-based intelligent intersection control algorithms. Third, the fuel consumption and emissions model take into account the fuel production, processing and delivery emissions. Fourth, a simulated hierarchical four-layered structure is applied in the wireless communication system (CS).

Related work

Suthaputchakun, Zhili, and Dianati (2012) present a survey of the fuel efficiency and CO_2 emissions reduction based on vehicular communications as well as the envisaged technical challenges in this research area. The studies addressing strategies for fuel efficiency and CO_2 emissions reduction can be divided into the following main categories:

1. Traffic reduction and transportation hardware improvements;
2. Vehicle speed control and traffic signal management;
3. Reservation-based ITM.

Traffic reduction can be achieved through improved city planning, with major places within walking distance; public transportation improvement and through the promotion of carpooling and car sharing. These strategies can indirectly reduce fuel consumption and CO_2 emissions (Suthaputchakun et al., 2012).

Transportation hardware improvements can also contribute to fuel consumption and CO_2 emission reductions through improvements in infrastructure design (e.g., road paving materials and slope elimination) and vehicles (e.g., engine electronics, periodical vehicle checks).

Table 1 lists some prominent recent studies including the tools that were used. The emission models column

Table 1. Studies on vehicle emissions reduction through the use of reservation-based ITM.

Emission model	Scenario type	Algorithm	Results/Contributions
N/A	ST-4	Reservation-based approach based on a detailed communication protocol	Reservation-based approach significantly outperform current intersection control technology-traffic lights and stop signs (Dresnor & Stone, 2008)
HBEFA	ST-5	Priority-based policy, with-lane-based policy, first come, first serve	Reduced significantly the fuel consumption and vehicle emissions compared to traditional signal control systems (Qiu, Guoyuan, Boriboonsomsin, & Barth, 2012)
CMEM	VISSIM	Dynamic hierarchical reservation protocol	Assigning different priorities to incoming reservation requests; evaluation of the benefits from a mobility and an environmental point of view (Shan, Sadek, & Yunjie, 2012)
VT-CPFM	iCACC tool	Heuristic non-linear optimization	Optimization of vehicle trajectories to prevent vehicle collisions and minimize the total intersection delay (Wojtowicz, & Wallace 2010)

presents the instantaneous vehicle emission models applied in each study. These models can be divided into:

- Emission map-based models (e.g., HBEFA) – values for the speed, power, and fuel consumption are calculated using the so-called engine maps.
- Data-driven statistical based models (e.g., VT-Micro) – these models are built upon vehicle speed/acceleration and emission datasets (Park, Rakha, Farzaneh, Zietsman, & Lee, 2010).
- Physical based model [e.g., CMEM, EMIT, and VT-CPFM (Zohdy & Rakha, 2016)] – the vehicle physical dynamics is simulated as well as the corresponding dynamic power flow and energy losses within the powertrain. Physical models are classified into forward-facing and backward-facing.
- Real-world experiments – fuel consumption is directly computed/estimated based on field measurements. A CAN bus data logger was used by Liimatainen (2011) to record the fuel consumption, while in Munoz-Organero and Magana (2013) work, the mass air flow and vehicle speed were recorded using an on-board diagnostic port OBD2.

The scenario type column presents the environment used in each study to model traffic dynamics. These scenario types can be divided into:

- Microscopic simulation (e.g., SUMO, VEINS, INTEGRATION, ST-4, ST-5, and VISSIM) – microscopic simulation environment provides a detailed representation of the traffic, and thus capture the behavior of vehicles and drivers with great detail;
- Mesoscopic simulation (e.g., DYNAMO) – models individual vehicles at an aggregate level, that is, individual vehicles are modeled but not their interactions;
- Macroscopic simulation – capture traffic dynamics of large networks, that is, model traffic as a continuous flow (Yang, Wang, & Yin, 2012);
- Real-world experiments – where data acquired for the analyzed scenario are taken from real-world experiments (Liimatainen, 2011; Munoz-Organero & Magana, 2013).

Additionally, the scenario type may include V2V/V2I communication simulators, namely OMNET, NS-2/3, NetSim, and NCTUNS, but they are often missed in most of the studies (Ferreira & Orey, 2012; Sommer, Krul, German, & Dressler, 2010). Vehicular fuel consumption and CO_2 emissions are proportional to the frequency of accelerations and decelerations. The majority of the studies attempt to reduce vehicle accelerations, decelerations, and avoid stops, by controlling the vehicle speed. The proposed methods for the control of the vehicle speed can be divided into two categories: direct and indirect methods. The direct speed control method can automatically control the vehicle speed or provide an eco-friendly speed advice to the driver (Liimatainen, 2011). The indirect speed control can make use of infrastructure variable speed limits or variable traffic light system (TLS) timings in order to comply with a low level of jerk along the path and reduce engine idling (Munoz-Organero & Magana, 2013; Yang et al., 2012). A more complex system is presented in Ferreira and Orey (2012), the proposed algorithm aggregates the control of several traffic signal systems (TLSs) timings, achieving significant CO_2 reductions.

A summary of studies on vehicle emission reduction through the use of reservation-based ITM is presented in Table 1. The reservation-based ITM was first proposed by Dresner and Stone (2008). The vehicles' pose were considered to be known, no emission model was considered and the V2I wireless communications were simulated through a basic protocol-less communication system. Qiu et al. (2012) developed a single lane crossroad intersection time-space occupancy reservation scheme. A Priority-based Policy, With-Lane-based Policy, First-come-first-serve (FCFS) algorithm was applied. The vehicles' pose were considered to be known and the V2I wireless communications were simulated through a basic protocol-less communication system. The proposed strategy reduced the vehicle fuel consumption and emission levels significantly compared to traditional signal control systems. Zohdy and Rakha developed a centralized intersection controller that optimizes the vehicle trajectories to minimize the total intersection delay, the algorithm was extended to operate on roundabouts where any failure in communication would have a traditional roundabout intersection control (Wojtowicz & Wallace, 2010), the assumption of an existent communication system was made and it was also assumed that the vehicles' pose was known *a priori*. A speed profile for each vehicle crossing an intersection was proposed by Shan et al. (2012) and applied in their integrated microscopic traffic simulator. An integrated framework was used to develop a dynamic hierarchical reservation-based ITM and to conduct studies of the environmental impacts of its application. The ITM algorithm assigns different priorities to incoming reservation requests. Results

revealed significant mobility benefits, in terms of increased capacity to handle traffic and reductions in fuel consumption, emission levels, and travel time. The communication layer used a basic protocol-less communications system to simulate V2I wireless communications and the vehicles' pose were considered to be known.

Intelligent traffic management system

When developing ITM algorithms, involving an improvement cycle of both models and algorithms under research, it is important to be able to conduct realistic microscopic simulation studies. This article analyzes the high potential in overall traffic performance enhancement at intersections by integrating an instantaneous emission computation module in a microscopic traffic simulator.

Simulator architecture

As shown in Figure 1, the ISR-TRAFSIM is composed of an Infrastructure Agent, Vehicle Agents, and a V2V/V2I Communication module.

1. Infrastructure Agent: The Infrastructure Agent is responsible for the selection of the algorithm that manages traffic at each intersection. If the selected algorithm is one of the following two: WMITM or the EMITM, the speed profile and navigational directions of each vehicle are computed (see the Section "Traffic management algorithms") and sent by the Infrastructure Agent to the Vehicle Agents. The vehicles' pose are updated on a spatiotemporal matrix, according to the routes and speed profiles computed by the selected management algorithm. Each intersection runs independently its own traffic management algorithm, and therefore, the performance can be evaluated separately.
    - Roundabout Intersection – The RI management system may function with one of the three traffic management algorithms: ITMD, WMITM, or the EMITM. The application on a RI of both the WMITM and EMITM algorithms is described in Bento et al. (2012a).
    - Crossroads Intersection – The CI management system may function with one of four traffic management algorithms: STLS, CIITM, WMITM, or the EMITM. The application on a CI of both the STLS and CIITM algorithms is described in Bento et al. (2012a).
2. Vehicle Agents: Vehicle Agents use the infrastructure road network and origin-destination (O-D) matrix to determine their routes. The vehicle's real speed and acceleration are used by the *Environmental Impact* module, every simulation cycle, for the computation of the fuel consumption, and CO_2 emissions. The emissions are computed using the thermal engine model described in the Section "Environment impact: emissions and fuel consumption computation". The vehicles' pose is

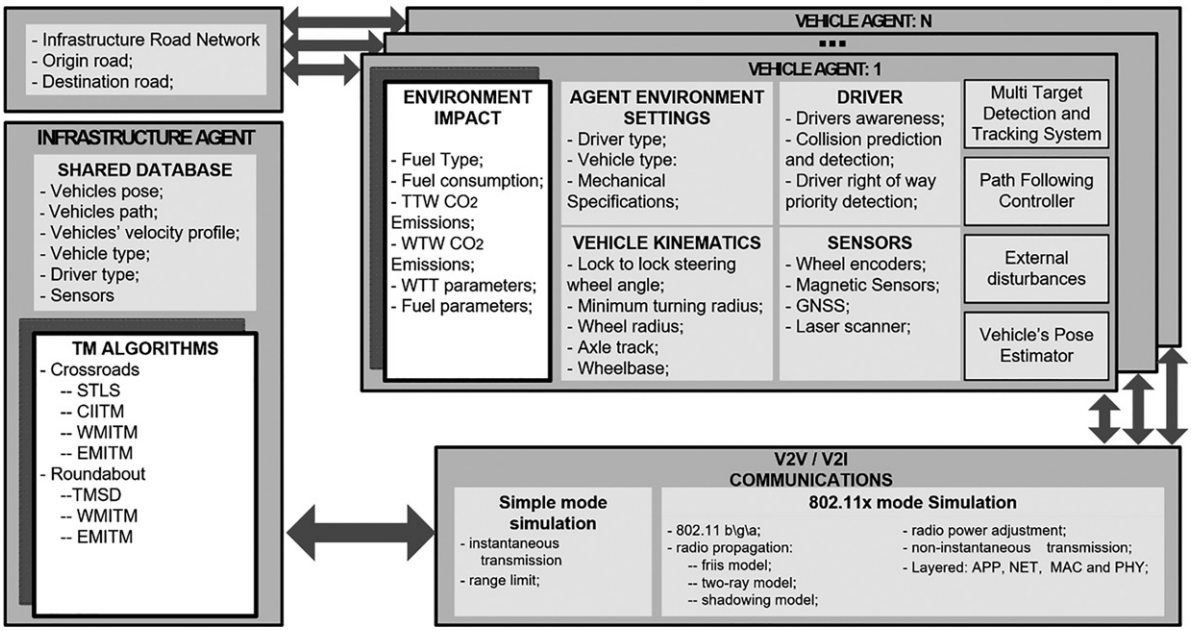

Figure 1. ISR-TRAFSIM simulator architecture.

estimated by fusing the information gathered from several simulated sources, namely GNSS and odometry (Bento, Parafita, & Nunes, 2012b). The simulated GNSS pseudoranges are affected by the following simulated sources of noise: ionospheric delay, tropospheric delay, multipath error, and thermal noise. Quantization effects were taken into consideration and Gaussian noise was added to the encoder readings, thus affecting the odometry pose estimation. Two other sources of noises were considered, namely independent Gaussian noises on the wheel to wheel distance and on the front to rear axle distance. Each vehicle while moving, outputs its estimated pose, speed, travel time, and the CO_2 emissions and fuel consumption levels.

A system for detection and tracking of moving objects using a simulated laser range finder, is constantly monitoring the vehicle surroundings and providing comprehensive analysis of the speed and direction of other vehicles (Mendes, Bento, & Nunes, 2004).

3. V2V/V2I Communications: The *V2V and V2I communications module* provides a secure channel for information exchange among vehicles and infrastructure (Zhou, Evans, Chowdhury, Wang, & Fries, 2011). In the ISR-TRAFSIM, an *IEEE802.11b/g/a* communication system (CS) is simulated (Ray, Carruthers, & Starobinski, 2005). The CS has a variety of features and configurable parameters, the most important are:
    - IEEE802.11b/g/a (CSMA/CA, NAV and RTS-CTS-DATA-ACK)
    - Three radio propagation models (Friis, two-ray ground, and log shadow)
    - SINR-based packet capture
    - Broadcast and ad-hoc routing

    The CS is implemented using four layers: an application layer (APP), a network layer (NET), a medium access control layer (MAC), and a physical layer (PHY). A receiver decodes a packet if and only if the, SINR during packet reception, is above the sensitivity defined for the receiver. The developed CS does not support a periodic beacon procedure such as in Palomar, Fuentes, Gonzalez-Tablas, and Alcaide (2012). The transmission of data frame is followed by a acknowledge (ACK) frame. Between a data frame and the ACK frame there is a short interframe space (SIFS). After the ACK frame, there is a distributed coordination function (DCF) interframe space (DIFS) followed by a contention window (CW), where CW is a value between [CW_{min}, CW_{max}]. A station that intends to transmit must sense an idle medium for a DIFS period then selects a backoff timer within a backoff window. The backoff timer is derived from a uniform distribution over the interval [0, CW]. The CW values are sequentially ascending integer powers of 2, minus 1. The backoff timer is decreased only when the medium is idle; it is frozen when another station is transmitting. Each time the medium becomes idle, the station waits for a DIFS period, and next starts continuously decrementing the backoff timer. As soon as the backoff timer expires, the station is authorized to access the medium and transmit. If some other station is already transmitting (it had a shorter random backoff interval), it will have to wait until after the next DIFS and go through the contention window again (Zhang, Yang, & Ma, 2008). The Network Allocation Vector (NAV) virtual carrier sensing mechanism was implemented to further reduce collisions. Both CI and RI have V2I modules, enabling each ITM to communicate with vehicles in the communication range. Communication between RI and CI is also available, enabling information handshaking of a vehicle crossing both zones.

The ISR-TRAFSIM road network layout includes two common solutions to regulate intersection traffic, roundabouts and crossroads as depicted in Figure 2.

Traffic management algorithms

ITM algorithms are important for achieving economic and environmental benefits. Three ITM algorithms were developed and are analyzed in this article. They can be divided in two categories: (i) space reservation-based schemes – CIITM; (ii) spatiotemporal reservation-based schemes (see Figure 3) – WMITM and EMITM. In addition, two traditional strategies of traffic regulation are considered: ITMD and STLS.

Intelligent traffic management deactivated (ITMD)

While on ITMD, vehicles respecting traffic laws and interacting with surrounding vehicles, follow their auto-generated path and speed profile. There is no predefined speed profile and the speed is determined at each time interval using a longitudinal inter-vehicle gap speed model and a transversal time to collision algorithm. In this mode, vehicles crossing the intersection do not require a V2V/V2I communication system for proper operation.

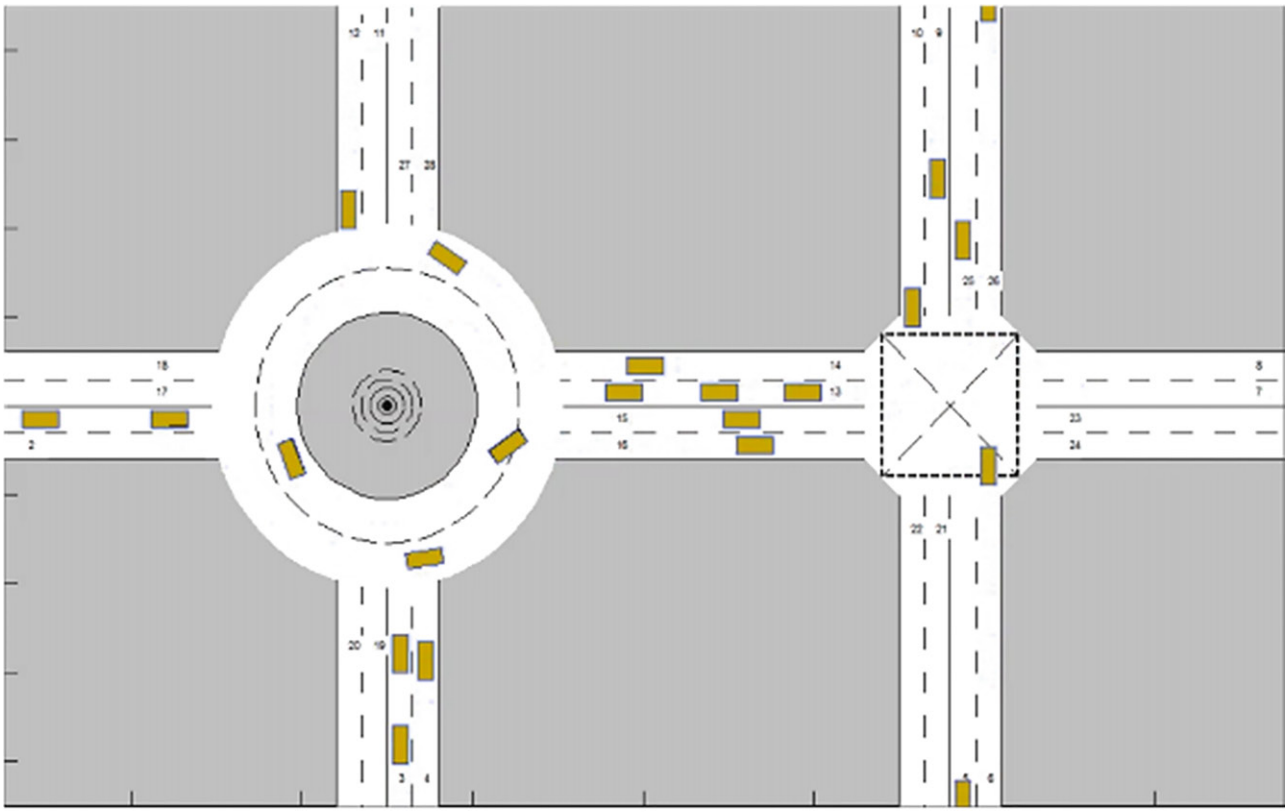

(a)

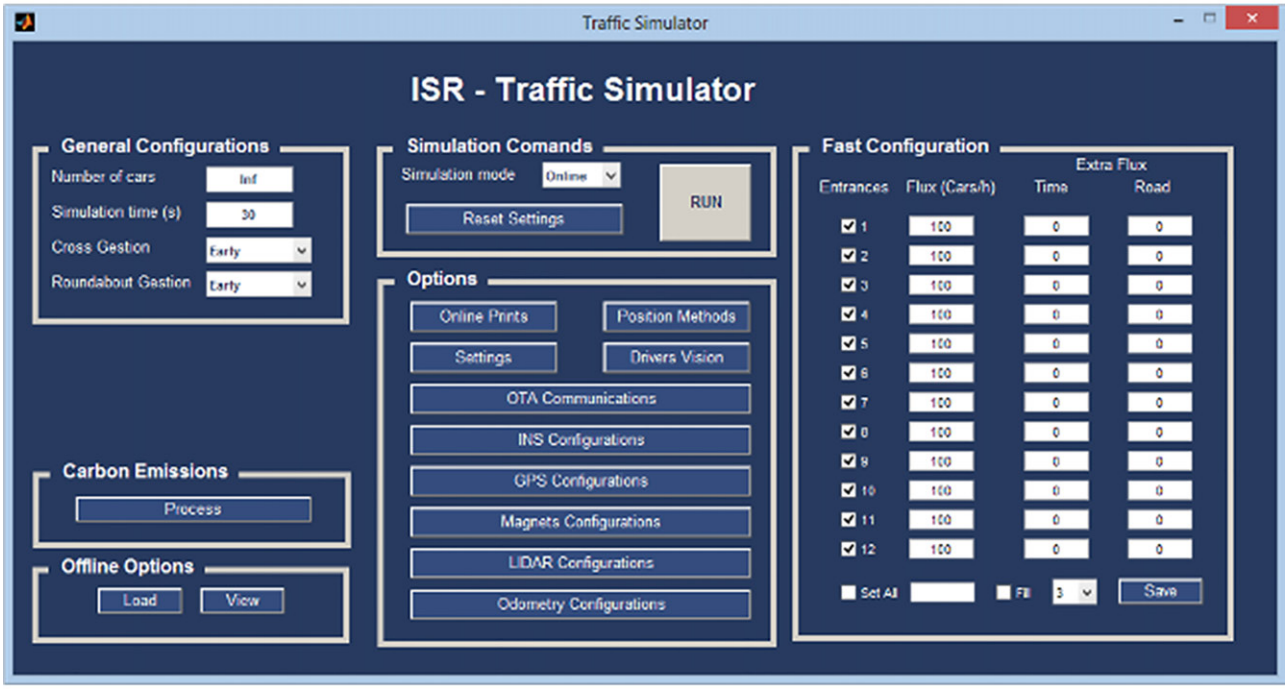

(b)

Figure 2. Simulator main interfaces: (a) scenario interface populated by car like vehicles, (b) configuration interface.

Standard traffic light system (STLS)

In STLS mode of operation, it was considered a fixed-time control strategy, with a phase serving each direction at a time. Regardless of changes in traffic volumes, the STLS uses the same preset in every cycle. A full cycle length for one direction is composed of $T_{dir} = T_{green} + T_{yellow} + T_{red}$; during T_{dir} all other directions are in red light status. A full intersection cycle is composed by $T_{inter} = 4 \cdot T_{dir}$. During T_{red} all intersection traffic lights are red, enabling vehicles to

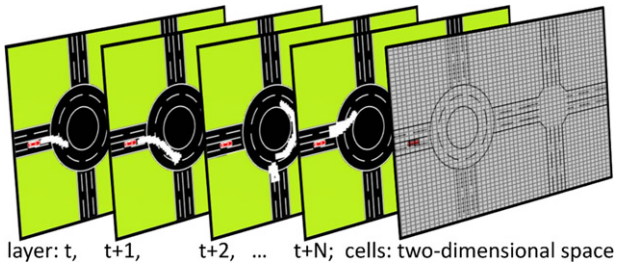

Figure 3. 3D matrix spatiotemporal matrix: 3D matrix representing a 2D (*x* and *y* space), plus a time dimension. The reservation is done on both space and time building a speed profile and reservation space for each vehicle traversing the scenario.

clear the intersection safely. The STLS system does not require a V2V/V2I communication system, neither the vehicles crossing the intersection.

Crossroad intersection intelligent traffic management (CIITM)

Using the infrastructure sensors to detect incoming and outgoing traffic, the CIITM manages the intersection using a space allocation algorithm. In addition to the traffic lights, the intersection is assumed to be equipped with an intelligent vision system and road drive-through inductive loop sensors. The intelligent vision system, assumed to be present on the infrastructure, must detect the approaching vehicles and check the status of the turning light signals of each vehicle. A set of drive-through inductive loop sensors in each outgoing lane are capable of detecting the vehicles leaving the intersection. The management process occurs in three stages: (1) detection of intended turning behavior; (2) verification of the status (free/occupied) of the path and outgoing lane, assigning green or red traffic light to the corresponding lane accordingly; (3) detection of the vehicle passage at the output lane and release of the allocated space for usage of following vehicles. The pseudo-code of the CIITM is presented in Algorithm 1.

Algorithm 1: Crossroad Intersection Intelligent Traffic Management (CIITM)

Require: spatiotemporal matrix, vehicle origin, vehicle destination, inward sensors, outward sensors

Use inward sensors to determine destination and compute trajectory path
if destination and trajectory path free **then**
    Reserve cell(x,y) in the spatial matrix
    while vehicle not crossed traffic light **do**
        Set green light
    end while
        Set red light
else
        Added to DATABASE QUEUE of cars
end if
if outward sensors detection **then**
        Release cell(x,y) in the spatial matrix
end if

This algorithm does not require a V2V/V2I communication system, relying solely on infrastructure sensors to detect incoming, outgoing traffic, and intended turning behavior; therefore, reducing costs. If the infrastructure does not recognize the intended turning behavior of the vehicle, then a hazardous event might occur.

Early method intelligent traffic management (EMITM)

If a vehicle is inside a predetermined intersection control radius, this algorithm generates a collision-free path. The collision-free path is decomposed into a speed profile along with navigational directions. The speed profile and navigational directions are sent only once, therefore, the success of this algorithm relies on the important premise that the vehicle follows the recommendations precisely. This method is based on a spatiotemporal matrix reservation scheme (see Figure 4). The reservation process starts with a path generation based on the vehicle's current estimated pose and destination lane. Using the determined path and the preferred speed defined by the *environmental agent settings*, a speed profile is computed. The generated path and speed profile is used in the reservation procedure applied to the spatiotemporal matrix. If there is a potential reservation conflict, the speed profile is recalculated so that the vehicle waits until the first free space is found. This collision avoidance reservation process is repeated until an origin-to-destination collision-free path is obtained. Once the collision-free path is obtained, the final speed profile along with navigational directions are sent to the respective vehicle. The cells reserved in the spatiotemporal matrix are wider than the vehicle dimensions; this configurable parameter A_{safety} is a safety measure used to avoid collisions, in case, the vehicle does not follow the generated speed profile precisely. The parameter A_{safety} also accounts for the error-prone positions, that is, it must be increased for less accurate vehicle pose estimations. This algorithm relies on a V2V/V2I communication system to receive the vehicle's current estimated pose and destination lane and to send the speed profile and the navigational directions.

The EMITM pseudo-code is presented in Algorithm 2. The EMITM algorithm has roughly the

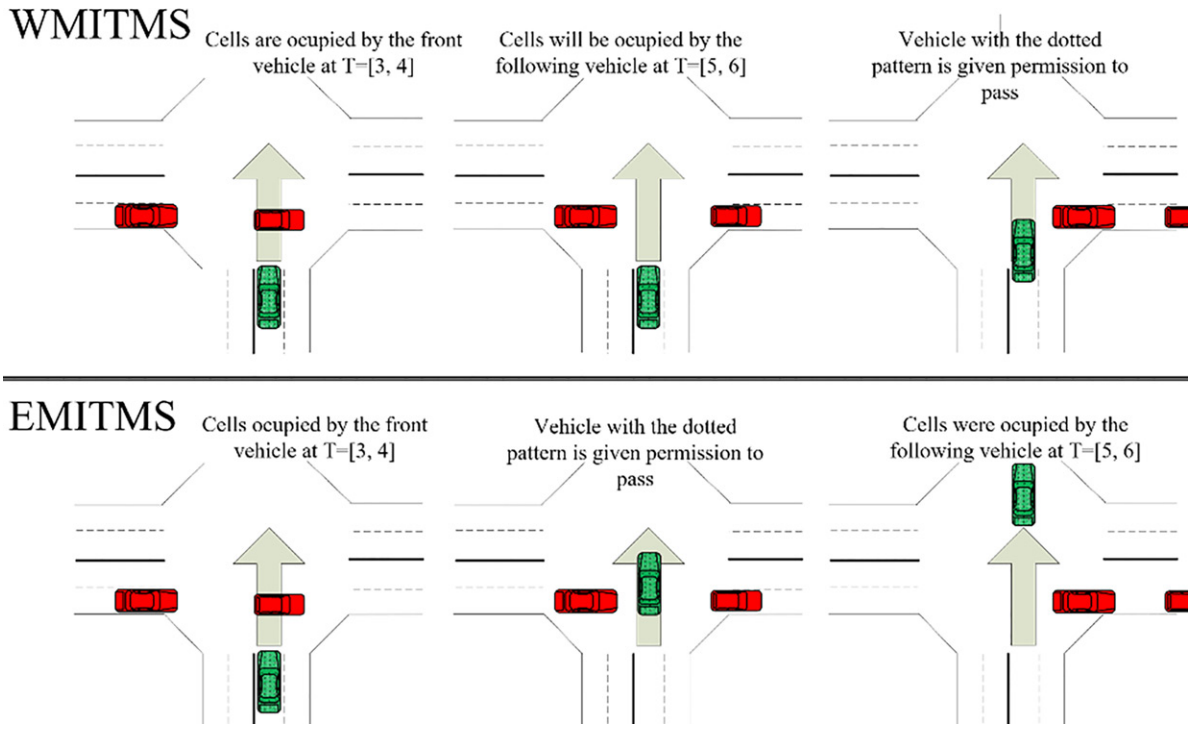

Figure 4. Cell selection using {\emph waiting} and {\emph early} algorithm. The EMITM algorithm reserves the space as soon as it is available, while WMITM algorithm determines that a vehicle must wait until the space required is no longer used.

same operation as a previously developed algorithm, the *Waiting method intelligent traffic management* (WMITM) (Bento et al., 2012a).

The main difference is that in conflicting situations the EMITM will try to reserve the first free space, while the WMITM will try to reserve the immediate free space after the last reserved space, for example, if the algorithm attempts to reserve a cell at T = 3s and the cell was occupied between the following time intervals $T = [3; 4]U, [5; 6]$, the speed profile generated by EMITM will determine that the vehicle has to slow down until the instant just after T = 4 s while the WMITM will determine to decrease the speed of the vehicle until the instant immediately after T = 6 s, see Figure 4. This is the major difference between the two algorithms.

Algorithm 2: Early Method Intelligent Traffic Management (EMITM)

Require: spatiotemporal matrix, vehicle V2I/V2V communication, vehicle origin, vehicle destination

Use origin and destination to generate trajectory path
if destination free **then**
  Set obstacles list to empty
  while unsuccessful reservation **do**
    Use trajectory and obstacles list to generate the speed profile
    Use speed profile and spatiotemporal matrix to detect collisions
    if collisions **then**
      Find layer(i) and cell(x,y) of the spatiotemporal matrix with collision
      Use detected occupied cell(x,y) of the layer(i) to update obstacles list
      Compute speed profile delaying the arrival time to cell(x,y) until layer(i)
    else
      Update spatiotemporal matrix
      successful reservation
    end if
  end while
  Send speed profile to vehicle V2I/V2V address
else
  Send waiting signal to vehicle V2I/V2V address
end if

Environment impact: emissions and fuel consumption computation

ISR-TRAFSIM includes a newly developed module that computes CO_2 emissions as well as the fuel consumption of the vehicles traversing the intersections, based on an engine thermal model and the vehicle longitudinal dynamics. The engine power output and speed from physical interrelationships are computed as follows: the force required to accelerate the vehicle is calculated directly from the required linear speed

which is translated into a rotational speed. To compute the fuel needed to meet speed requirements, the required force is translated into the torque that must be provided, when a rotational force is applied to a shaft. This approach is called *quasistatic* or *backward-facing* where, assuming that the vehicle follows a required speed, we compute how each component must perform (Wipke, Cuddy, & Burch, 1999). Component-by-component, this calculation approach flows backward through the drivetrain, against the tractive power flow direction, until the required fuel use to meet the speed profile is computed. The backward-facing approach can compute the emissions and fuel consumption of any speed profile and has the advantage of low computing requirements. The implemented backward-facing approach is presented in Algorithm 3.

Vehicle mechanical model

The model of the vehicle is based on the mechanical forces acting on the vehicle. In order to compute the vehicle fuel consumption, the required power must be computed taking into account its physical dependencies\cite{ref:willans_appr}. Considering a vehicle as a mass-point, its equilibrium equation can be written as follows:

$$F_{\text{trac}} = \text{F}_{\text{roll}} + F_{\text{aero}} + F_{\text{inertia}} + F_{\text{grade}} \tag{1}$$

where, F_{trac} is the resulting tractive force at the wheels to move the vehicle forward, F_{roll} is the rolling resistance, F_{aero} is the force due to aerodynamic drag, F_{inertia} is the inertial force, and F_{grade} is the force due to road slope. Rolling resistance is associated with the friction due to tire deformation as wheels rotate. The equation for rolling resistance is given by

$$F_{\text{roll}} = m_{\text{veh}} \cdot g \cdot C_{\text{R}} \tag{2}$$

Where, m_{veh} is the total vehicle mass, g is the gravity acceleration, and C_{R} is the coefficient of rolling resistance. The aerodynamic drag force is given by

$$F_{\text{aero}} = 1/2 \cdot \rho_{\text{air}} \cdot A_{\text{f}} \cdot C_{\text{D}} \cdot \overline{v}_{\text{veh}}^2 \tag{3}$$

where, ρ_{air} is the air density, A_{f} is the vehicle frontal area, C_{D} is the vehicle aerodynamic drag coefficient, and v_{veh} is the vehicle speed. The drag force must be calculated with the mean speed in every time step interval, that is, $\overline{v_{\text{veh}}}$. The inertial force is the load due to the acceleration of the vehicle's mass and it is given by

$$F_{\text{inertial}} = m_{\text{veh}} \cdot \dot{v}_{\text{veh}} \tag{4}$$

The component of the vehicle weight opposing the motion of the vehicle defines the grade force

$$F_{\text{grade}} = m_{\text{veh}} \cdot g \cdot \sin(\alpha) \tag{5}$$

where, α is the angle of the road from horizontal. In this article, the road is assumed to be flat, therefore, α is always zero.

Thermal engine model

The traction force F_{trac} has to match the total resistance force (1) for every time step in the discrete speed profile (Guzzella & Onder, 2004). Once obtained the F_{trac}, the first step to compute the necessary engine torque is to calculate the engine rotational speed, ω_{eng}, using the wheel radius, r_{wheel}, and the gear ratio, γ:

$$\omega_{\text{eng}} = \frac{\overline{v}_{\text{veh}}}{r_{\text{wheel}}} \cdot \gamma \tag{6}$$

where, the gear ratio γ is function of $\overline{v_{\text{veh}}}$. In order to comply with the determined vehicle speed, the engine must apply the following torque T_{eng} to the crankshaft:

$$T_{\text{eng}} = \frac{F_{\text{trac}}}{\omega_{\text{eng}}/\overline{v}_{\text{veh}}} \tag{7}$$

The Willans approximation (Guzzella & Sciarretta, 2005) for the engine's torque and efficiency characteristics was used:

$$\rho_{\text{me}} = \epsilon \cdot \rho_{\text{mf}} - \rho_{\text{me0}} \tag{8}$$

where, ρ_{me} is the brake mean effective pressure, ϵ is the indicated engine efficiency, ρ_{mf} is the fuel mean effective pressure, and ρ_{me0} represents all mechanical friction and pumping losses. The Willans approximation was chosen because it provides a low computation model while it models very well real engine behavior.

Algorithm 3: Emissions and Fuel Consumption

Require: Vehicle Mechanical specifications, Engine Specifications, Fuel Characteristics, vehicle Speed

→ Use vehicle Speed and Vehicle Mechanical Specifications to compute the Required Traction Force

$$F_{trac} = m_{veh} \cdot g \cdot C_R + 1/2 \cdot \rho_{air} \cdot A_f \cdot C_D \cdot \overline{v_{veh}^2} + m_{veh} \cdot \dot{v_{veh}} + m_{veh} \cdot g \cdot \sin(\alpha)[N]$$

if $F_{trac} > 0$ then

→ Use vehicle Speed and Gear Ratio to obtain Rotational Speed: $\omega_{eng} = \frac{\overline{v_{veh}}}{r_{wheel}} \cdot \gamma[rad/s]$

→ Use the Required Traction Force, the Rotational Speed and the vehicle Speed to obtain Required Torque: $T_{eng} = \frac{F_{trac}}{\omega_{eng}/\overline{v_{veh}}}[Nm]$

→ Use the Required Traction Force and the engine displacement to obtain brake mean effective pressure: $\rho_{me} = \frac{T_{eng} \cdot N \cdot \pi}{V_d} [bar]$

Applying the engine friction model compute the engine friction losses:

$$\rho_{me0f} = k_1 \cdot \left(k_2 + k_3 \cdot S^2 \cdot \omega_{eng}^2\right) \Pi_{max} \cdot \sqrt{\frac{k_4}{B}} [bar]$$

→ Use friction losses and global engine losses to obtain global engine losses: $\rho_{me0} = \rho_{me0g} + \rho_{me0f} [bar]$

→ Use the brake mean effective pressure, the global engine losses and the indicated engine efficiency to obtain fuel mean effective pressure: $\rho_{mf} = \frac{\rho_{me} + \rho_{me0}}{\epsilon} [bar]$

switch (Fuel Type)

case Gasoline:

$$H_l^{fuel} = H_l^{C_8H_{18}} [MJ/kg]$$
$$\rho_{fuel} = \rho_{C_8H_{18}} [kg/l]$$
$$N_{molecules}^{CO2} = 8$$
$$M_{fuel} = M_{C_8H_{18}}$$
$$WTT_{fuel} = WTT_{C_8H_{18}}^{CO_2}$$

case Ethanol:

$$H_l^{fuel} = H_l^{C_2H_5} [MJ/kg]$$
$$\rho_{fuel} = \rho_{C_2H_5} [kg/l]$$
$$N_{molecules}^{CO2} = 2$$
$$M_{fuel} = M_{C_2H_5}$$
$$WTT_{fuel} = WTT_{C_2H_5}^{CO_2}$$

end switch

→ Use the fuel mean effective pressure, the engine displacement and the fuel lower heating value to obtain fuel mass per engine cycle: $m_f = \frac{\rho_{mf} \cdot V_d}{H_l^{fuel}} [kg]$

→ Use vehicle fuel mass per engine cycle and Rotational Speed to obtain fuel mass flow:

$\dot{m}_f = m_f \cdot \frac{\omega_{eng}}{N \cdot \pi} [kg/s]$

→ Use vehicle fuel mass flow, the time interval, the fuel density and traveled distance to obtain fuel consumption:

$$FC_{100km} = \frac{\frac{\dot{m}_f \cdot \Delta t}{\rho_{fuel} \cdot 100}}{\frac{\Delta s}{1000}} [l/100km]$$

→ Use vehicle fuel consumption, the fuel density, the number of CO_2 molecules produced on the combustion process, the CO_2 molar mass and fuel molar mass to obtain $TTW_{fuel}^{CO_2}$ emissions:

$$TTW_{fuel}^{CO_2} = FC_{100km} \cdot \rho_{fuel} \cdot N_{molecules}^{CO2} \cdot \frac{\frac{M_{CO_2}}{M_{fuel}}}{100} \cdot 1000 [gCO_2/km]$$

→ Use vehicle TTW fuel CO_2 emissions, the fuel consumption, the fuel density, the fuel lower heating value and the $TTW_{fuel}^{CO_2}$ to obtain $WTW_{fuel}^{CO_2}$ emissions:

$$WTW_{fuel}^{CO_2} = TTW_{fuel}^{CO_2} + FC_{100km} \cdot \rho_{fuel} \cdot H_l^{fuel} \times \frac{WTT_{fuel}}{100} [gCO_2/km]$$

else

Set $FC_{100km} = 0$, $TTW_{fuel}^{CO_2} = 0$ and $WTW_{fuel}^{CO_2} = 0$

end if

The brake mean effective pressure, ρ_{me}, is the pressure that has to act on the piston during one full expansion stroke to produce the same amount of work as the real engine does in two engine revolutions:

$$\rho_{\mathrm{me}} = \frac{T_{\mathrm{eng}} \cdot N \cdot \pi}{V_{\mathrm{d}}} \tag{9}$$

where, V_{d} is the engine's displacement and $N = 4$ for a four-stroke engine.

The fuel mean effective pressure, ρ_{mf}, is the brake mean effective pressure, that an engine with an efficiency of 100% would produce, by burning the fuel mass m_{f} per engine cycle, with a fuel lower heating value of H_{l} ($H_{\mathrm{l}}^{C_8H_{18}}$ is the lower heating of the gasoline and $H_{\mathrm{l}}^{C_2H_5}$ is the lower heating of the ethanol):

$$\rho_{\mathrm{mf}} = \frac{m_{\mathrm{f}} \cdot H_{\mathrm{l}}}{V_{\mathrm{d}}} \tag{10}$$

The ρ_{me0} represents the engine's losses due to friction $\rho_{\mathrm{me0}f}$ and gas exchange $\rho_{\mathrm{me0}g}$:

$$\rho_{\mathrm{me0}} = \rho_{\mathrm{me0}g} + \rho_{\mathrm{me0}f} \tag{11}$$

The ρ_{me0f} follows a friction model as described in Guzzella and Onder (2004):

$$\rho_{\mathrm{me0}f} = k_1 \cdot \left(k_2 + k_3 \cdot S^2 \cdot \omega_{\mathrm{eng}}^2\right) \Pi_{\mathrm{max}} \cdot \sqrt{\frac{k_4}{B}} \tag{12}$$

where, S is the stroke, B is the bore, and $k_i \wedge i \in \{1, 2, 3, 4\}$ are constants of the friction model defined

in Guzzella and Onder (2004). The maximum boost ratio, Π_{max}, is 1 for naturally aspirated engines.

Fuel consumption and emissions computation

Using (Equations (8) to (12)), one can compute the fuel mass flow:

$$\dot{m}_f = m_f \cdot \frac{\omega_{eng}}{N \cdot \pi} \tag{13}$$

The total fuel consumed is the summation of the fuel consumption at each time interval Δt as long as the required F_{trac} is positive. Two types of fuel consumption were analyzed in this article: gasoline and ethanol. The chemical equation for the combustion (Pinkerton & Herbst, 2010) of gasoline is:

$$C_8H_{18} + 12.5O_2 \longrightarrow 8CO_2 + 9H_2O \tag{14}$$

and for ethanol, it is:

$$C_2H_5OH + 3O_2 \longrightarrow 2CO_2 + 3H_2O \tag{15}$$

The burning process of the gasoline and ethanol results in emissions of 8 and 2 molecules of CO_2, respectively.

Given the number of CO_2 molecules produced by the combustion and the molar mass of the gasoline ($M_{C_8H_{18}}$), ethanol ($M_{C_2H_5}$), and CO_2 (M_{CO_2}), one can compute the tank to wheel (TTW) CO_2 grams emission for gasoline (Johnson, 2008):

$$TTW_{C_8H_{18}}^{CO_2} = \sum \left(\dot{m}_f \cdot \Delta t\right) \cdot \rho_{C_8H_{18}} \cdot 8 \cdot \frac{M_{CO_2}}{M_{C_8H_{18}}} \tag{16}$$

and for ethanol:

$$TTW_{C_2H_5}^{CO_2} = \sum \left(\dot{m}_f \cdot \Delta t\right) \cdot \rho_{C_2H_5} \cdot 2 \cdot \frac{M_{CO_2}}{M_{C_2H_5}} \tag{17}$$

where, $\rho_{C_8H_{18}}$ and $\rho_{C_2H_5}$ are the gasoline and ethanol densities, respectively. Using the well-to-tank CO_2 emissions (WTT^{CO_2}) and Equations (16) and (17), one can compute the well-to-wheel CO_2 emissions for gasoline (Alvarez, Martinez, & Franco, 2013; Edwards, Larive, & Beziat, 2011):

$$WTW_{C_8H_{18}}^{CO_2} = TTW_{C_8H_{18}}^{CO_2} + \sum \left(\dot{m}_f \cdot \Delta t\right) \cdot \rho_{C_8H_{18}} \times H_l^{C_8H_{18}} \cdot WTT_{C_8H_{18}}^{CO_2} \tag{16}$$

and for ethanol:

$$WTW_{C_2H_5}^{CO_2} = TTW_{C_2H_5}^{CO_2} + \sum \left(\dot{m}_f \cdot \Delta t\right) \cdot \rho_{C_2H_5} \times H_l^{C_2H_5} \cdot WTT_{C_2H_5}^{CO_2} \tag{16}$$

The developed algorithm for total fuel consumed and CO_2 emissions is presented in Algorithm 3.

Simulation results

The developed traffic simulator is highly customizable making it suitable not only for the analysis of ITM algorithms, fuel consumption and CO_2 emissions but as well for other ITS studies (e.g., sensor fusion; Bento et al., 2012b).

Simulation environment

The simulated road layout under study is composed by a roundabout and a crossroad intersection (see Figure 2). The traffic is right-handed, that is, vehicles on the RI travel anticlockwise, and no overtaking maneuvers are considered in this study. The RI traffic inflow/outflow arrives from four directions. Each direction is composed of two roads of inflow/outflow and each road has two lanes; the same setup is also applied to the CI. The CI can be controlled by traffic lights, and inside the CI box junction, vehicles are not allowed to stop, that is, a vehicle must not enter the box junction if there is no space for the entire vehicle to exit in the other side of the CI. The simulated vehicles run on gasoline or ethanol and are equipped with a four-stroke Otto cycle engine. The modeled engine is equipped with a *deceleration fuel cut off system* (DFCO) and a *start-stop system* (ST-SP). The DFCO detects if the car is coasting and then cuts fuel to the engine and allows the wheels to keep the engine running, which means that the car doesn't consume any fuel, when the power at the wheels is smaller or equal to zero. The ST-SP system automatically shuts down the engine when the vehicle stops and restarts it when power is required, this system reduces the engine idling time, and thereby reduces the fuel consumption and emissions. With this scenario, we are able to simulate complex vehicle/traffic situations; and thus, one can evaluate the impacts of different ITM strategies. The traffic densities simulated are presented in Table 2.

The results presented here refer to a 10-min time interval. The *Influx* column of Table 3, shows the number of vehicle agents to be created according to the traffic flow, for example, a total of $VA_{TFP} = 600$ vehicle agents should be created during 10 min on a scenario composed of a RI + CI (12 lanes input) for the $TFP3 = 300$[v/h/lane]:

$$VA_{TFP} = 300[\text{v/h/lane}] \cdot \frac{10[\text{min}] \cdot 60[\text{s}]}{3600[\text{s}]} \cdot 12[\text{lanes}] = 600[\text{vehicles}] \tag{16}$$

The simulation starts with a scenario without vehicles. For each lane, the vehicles' agents are created

Table 2. Number of vehicle agents (VA_{TFP}) that should be created during 10 min for each of the Traffic Flow Profiles (TFP) and each of the tested scenarios.

TFP	TFP1	TFP2	TFP3	TFP4	TFP5	TFP6	TFP7	TFP8	TFP9	TFP10	TFP11	TFP12	TFP13	TFP14
(veh/h/lane)	100	200	300	400	500	600	800	1000	1200	1600	2000	2400	3000	3600
RI or CI (8 input lanes)														
VATFP	134	267	400	534	667	800	1067	1334	1600	2134	2667	3200	4000	4800
RI + CI (12 input lanes)														
VATFP	200	400	600	800	100	1200	1600	2000	2400	3200	4000	4800	6000	7200

Table 3. Traffic, fuel consumption, and CO_2 emissions analysis simulation Test $i \wedge i \in \{1.18\}$, results for 10 min duration.

Case study		Cars influx		
Roundabout	Crossroads	100 vehicles/h/lane	200 vehicles/h/lane	300 vehicles/h/lane
ITMD	STLS	Test 1	Test 2	Test 3
EMITM	STLS	Test 4	Test 5	Test 6
ITMD	CIITM	Test 7	Test 8	Test 9
ITMD	EMITM	Test 10	Test 11	Test 12
EMITM	CIITM	Test 13	Test 14	Test 15
EMITM	EMITM	Test 16	Test 17	Test 28

Table 4. Vehicle origin-destination probability distribution.

Origin \ Destination	L_1	L_2	…	L_m
L_1	P_{11}	P_{12}	…	P_{1m}
L_2	P_{21}	P_{22}	…	P_{2m}
…	…	…	…	…
L_n	P_{n1}	P_{n2}	…	P_{nm}

Table 5. Communication system parameters.

IEEE 802.11a	
RXTX Turnaround= 2 (μs)	MAC header =34 (Byte)
SlotTime =9 (μs)	Max. payload =2312 (Byte)
CCA =4 (μs)	RTS =20 (Byte)
SIFS =16 (μs)	CTS = ACK =14 (Byte)
DIFS =24 (μs)	$CW_{min} = 15$
RX SINR threshold =10 (dB)	$CW_{max} = 1023$
TX power =0.2 (W)	RREQ = RREP =22 (Byte)
Receiver antenna gain =1	RREQ timeout =0.2 (s)
Transmitter antenna gain =1	RREQ max retries =3
Frequency =5(GHz)	Time To Live (TTL) = 7

Table 6. Vehicle origin-destination probability distribution from all lanes to lane 22.

Origin \ Destination	…	L_{22}	…
L_1	…	20%	…
L_2	…	20%	…
L_3	…	16%	…
L_4	…	33%	…
L_5	…	–	…
L_6	…	–	…
L_7	…	–	…
L_8	…	–	…
L_9	…	–	…
L_{10}	…	25%	…
L_{11}	…	20%	…
L_{12}	…	20%	…
…	…	–	…

Lane numbering is marked on Figure 8.

according to the defined *Traffic Flow Profile*. Each vehicle origin-destination lane setup, follows a semi-random model, as presented in Table 4, where P_{ij} represents the probability of a vehicle from an origin lane i to have its destination on lane j. The probability of a road to have more outflux than influx can be observed on Table 6, where the sum of the probability distribution from all lanes to lane 22 is more than 100%. Regarding the communication system, the IEEE802.11a protocol was chosen along with the Friis radio propagation model. We assume that all transmissions experience the same path loss versus distance profile, that every node transmits with the same power in the same channel, that the propagation delay is negligible and that each node has the same antenna gain and receiver sensitivity. The parameters used in simulation are presented in Table 5. Following the method presented in Koonce et al. (2008), when using STLS mode, the fixed time traffic lights are set to: $T_{green} = 15$ [s], $T_{yellow} = 5$ [s], and $T_{red} = 2$ [s]. The extra reserved area for safety purposes was set to $A_{safety} = [1.5;3][m]$. A_{safety} can be increased or decreased, function of the positioning accuracy and of the autonomous path following controller efficiency (Nunes & Bento, 2007).

ITM systems assessment

The simulations tests, where RI is running the *ITMD* and CI is running *STLS*, serve as reference for a performance evaluation of the other algorithms. As described in Bento et al. (2012a) the *EMITM* outperforms the *WMITM* when applied at RI, therefore, we have excluded the *WMITM* from the analysis in this article. The application on a RI of both *WMITM* and *EMITM* strategies are fully described in Bento et al. (2012a). To better access the algorithms performance two new scenarios were tested: first scenario

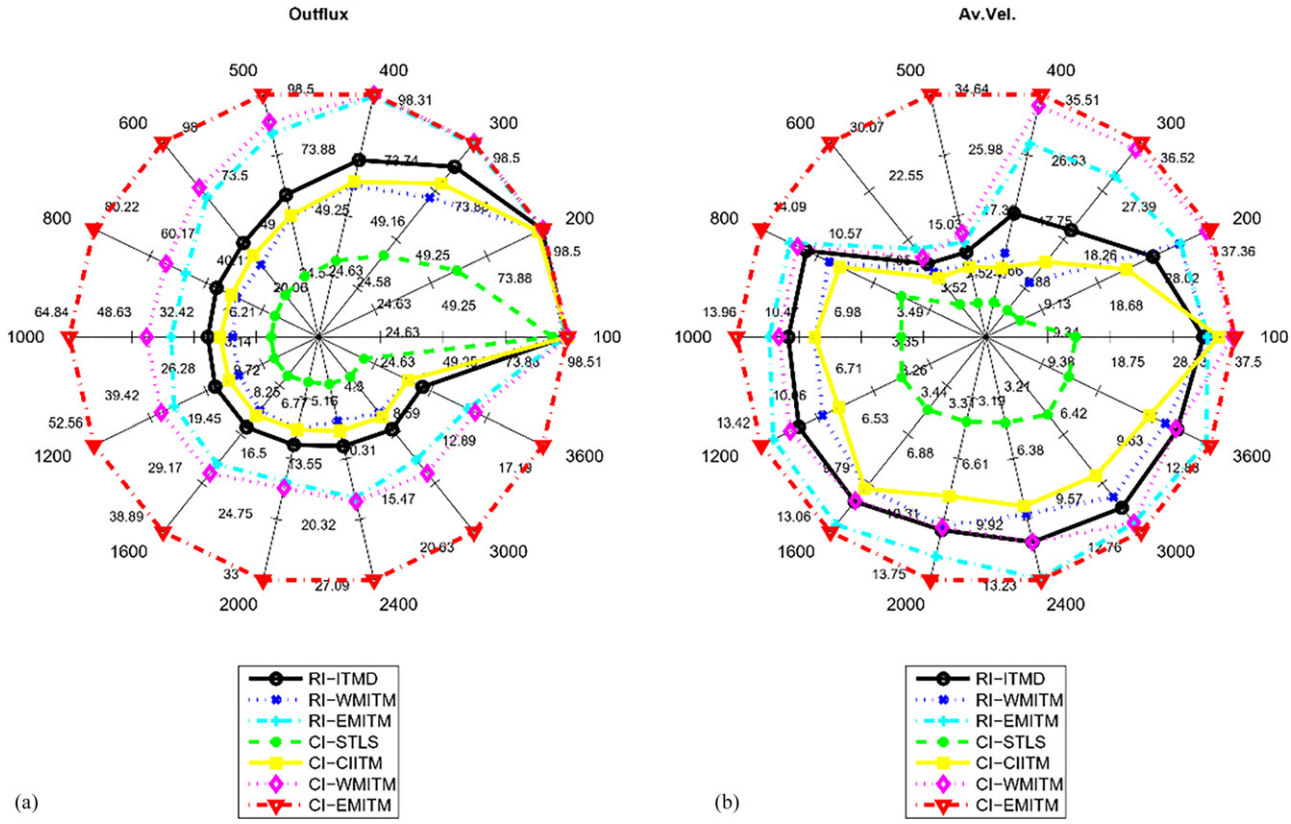

Figure 5. ITM results for an intersection composed of a RI or a CI: (a) Outflux[%]; (b) Av.Vel.[km/h]. Each axis line (starting in the center and extending to the periphery of the circle) represents TFP ranging from 100 to 3600 vehicles/hour/lane. For better graph readability, each axis line has different quantitative scales, for example, on subplot (a) the TFP1 (100 veh/h/lane) scale, ranges from 0% to 98.51%, while for the TFP14 (3600 veh/h/lane) scale, the range is from 0% to 17.19%.

composed of a single CI, second scenario composed of a single RI. The comparative evaluation of ITM algorithms in these two scenarios, can be better accessed in Figure 5. Figure 5 presents a subset of relevant analysis metrics, namely the *Outflux* (Figure 5a) and the Average Velocity *AV.Vel.* (Figure 5b). The *EMITM* algorithm evidenced the best results in both RI and CI intersections. For the same algorithm, the CI has a better performance than the RI. When a CI is regulated by the *EMITM*, the *Outflux*, is around 25% higher than the second-best algorithm for values of *Influx* above TFP7 (800 veh/h/lane). In Figure 6(a–c), the spatiotemporal matrix reservation for a multiple vehicle cells resource competition is presented. Figure 6(b) and (c) show the results of the application of the *EMITM* for the RI and CI, respectively, while Figure 6(a) shows the results of both RI and CI using their own independent EMITM.

The ITM algorithms where extensively simulated using 18 test runs, each test is characterized in Table 7. A major part of the data collected during the 10 min simulation is summarized in Table 3, where "*Influx*" is the number of vehicle agents that should have been created during the simulation, according to the traffic flow assigned for the Test; "*Created*" is the number of vehicle agents that were created during the simulation; "*Waiting*" is the number of vehicle agents that are waiting to be created at the end of the simulation, due to the lack of space on the scenario; "*Active*" is the number of vehicle agents still active and traversing the scenario at the end of the simulation and "*Exited*" is the number of vehicle agents that already traversed and exited the intersections scenario during the simulation. The number of vehicles waiting to be created increases with the increase of the traffic flow except when an ITM is applied in any intersection, this effect can be easily seen in the column "*output flux*" where the percentage is higher by applying the ITM. The "*output flux*" results of Tests 1–6, where STLS at the CI is used, are significantly lower than results of Tests 7–18, where a ITM at the CI is used, which means that the maximum number of vehicles traversing the intersections is limited by the performance of the CI. The previous hampering traffic

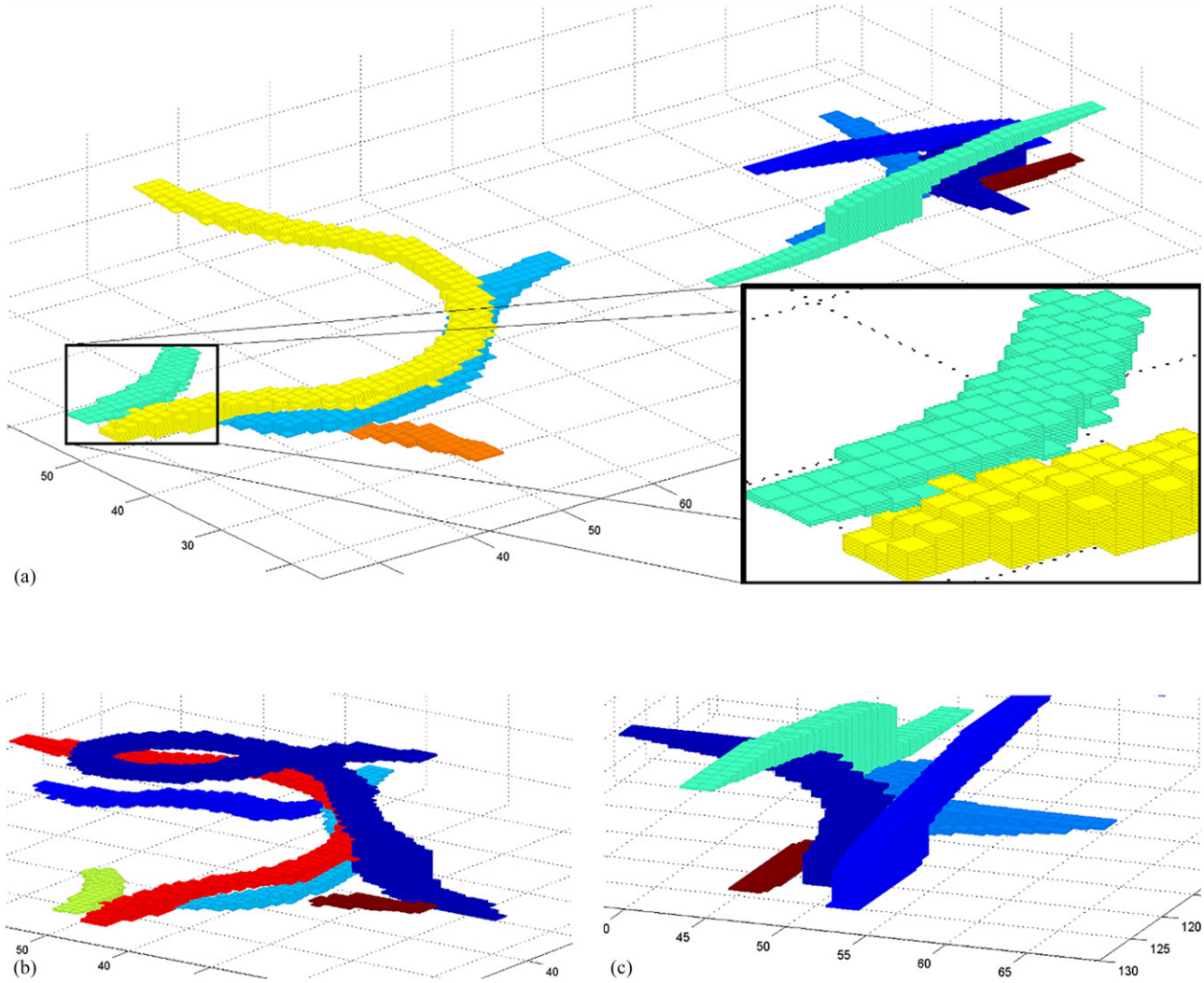

Figure 6. 3D spatiotemporal matrix reservation scheme for the EMITM applied to: (a) complete scenario, with the RI and CI running each its own management algorithm; (b) the roundabout; (c) the crossroad.

effect is easily seen in Figure 7, where even for the lowest tested traffic flow, TFP1, the speed profile for Test 1–6 is severely affected. The increase of the number of vehicles traversing the intersections occurs not only when the ITM systems are working together as well as if just one of them is working exclusively. The improved performance of an ITM is more noticeable when the traffic flux per lane is higher.

The CIITM outperforms traditional CI control techniques, which can be verified by comparing the results of Test 7–9 with Test 1–3 and results of Test 13–15 with Test 4–6. The EMITM when applied to both intersections, Test 16–18, is capable of increase the number of vehicles traversing the intersections compared to the use of any other tested combination of ITM algorithms. Figure 7 depicts this performance very well, the speed profile reduction for Test 16–18 is low, the immediate consequence is a higher "*mean speed*" (see Table 7).

Figure 8 presents the cell occupancy level for simulation Test 18, in this test, both intersections are regulated by the EMITM. Although in this test, the traffic inflow per lane is 300 cars/h, the level of occupancy is moderate and is slightly higher on approaching and inside of both intersections. This effect is compliant with the information presented in Figure 7, whereas the speed profile is moderately reduced before entering the RI and has a low reduction before entering the CI.

Environmental impact

Various simulation runs were conducted in order to quantify the potential benefits in fuel economy of the proposed ITM algorithms. The vehicle model is based on a mid-sized vehicle with mechanical specifications presented in Table 8 (Guzzella & Sciarretta, 2005). The fuel consumption and CO_2 emission results were

Table 7. Simulations tests catalog for each ITM, according to the traffic inflow of each of the 12 input lanes (RI and CI).

Vehicles			Traffic analysis						Gasoline			Ethanol		
	Influx	Created	Waiting	Active	Exited	Output flux [%]	Time stopped [%]	Mean speed [km/h]	Mean speed while in motion [km/h]	Mean consump. [l/100 km]	Mean TTW emiss. CO2 [gCO2/Km]	Mean WTW emiss. CO2 [gCO2-eq/Km]	Mean Consump. [l/100Km]	Mean TTW emiss. CO2 [gCO2/Km]	Mean WTW emiss. CO2 [gCO2-eq/Km]
Test 1	200	190	10	23	167	83.50	38.99	15.95	24.15	10.10	233.38	275.40	15.53	234.13	405.66
Test 2	400	300	100	53	247	61.75	47.91	9.82	17.92	12.97	299.88	353.88	19.96	300.85	521.25
Test 3	600	319	281	52	267	44.50	54.99	7.74	15.63	13.68	316.15	373.08	21.04	317.17	549.54
Test 4	200	193	7	24	169	84.50	41.45	14.77	23.26	10.32	238.64	281.62	15.88	239.41	414.81
Test 5	400	302	98	41	261	65.25	43.82	11.30	19.20	12.00	277.50	327.47	18.47	278.40	482.36
Test 6	600	317	283	48	269	44.83	55.37	8.52	17.34	12.36	285.83	337.30	19.02	286.75	496.83
Test 7	200	200	0	5	195	97.50	0.71	33.08	33.27	6.73	155.64	183.67	10.36	156.14	270.53
Test 8	400	374	26	19	355	88.75	11.40	25.09	27.36	9.60	221.88	261.84	14.77	222.60	385.68
Test 9	600	425	175	44	381	63.50	22.17	16.61	19.81	12.14	280.65	331.18	18.68	281.55	487.82
Test 10	200	200	0	5	195	97.50	0.46	30.49	30.62	9.16	211.73	249.86	14.09	212.41	368.03
Test 11	400	400	0	12	389	97.01	3.51	27.28	28.15	10.76	248.72	293.51	16.55	249.52	432.33
Test 12	600	539	61	45	494	82.33	13.10	16.75	18.63	13.53	312.86	369.19	20.82	313.87	543.81
Test 13	200	200	0	5	195	97.50	0.16	33.55	33.59	6.38	147.41	173.96	9.81	147.89	256.23
Test 14	400	371	29	22	349	87.25	8.27	27.47	28.75	8.71	201.24	237.47	13.39	201.89	349.79
Test 15	600	485	115	44	441	73.50	14.22	20.35	22.33	10.80	249.65	294.61	16.62	250.46	433.95
Test 16	200	200	0	5	195	97.50	0.22	35.00	35.06	5.29	122.22	144.23	8.13	112.62	212.45
Test 17	400	400	0	9	391	97.75	0.82	33.50	33.75	6.21	143.57	169.42	9.55	144.03	249.55
Test 18	600	600	0	15	585	97.50	2.01	31.20	31.77	7.42	171.53	202.41	11.42	172.08	298.15

obtained by simulating a naturally aspirated 1.5 L Otto cycle engine equipped with a 5-speed manual transmission. In this article, the gear-shift model efficiency and the engine simulation at cold-start were not taken into account.

The engine specifications and fuel characteristics are presented in Tables 9 and 10, respectively (Guzzella & Sciarretta, 2005; Safarianova, Noembrini, Boulouchos, & Dietrich, 2011; Wipke et al., 1999). In order to increase safety and to reduce fuel consumption and CO_2 emissions the speed limit in all scenario is set to 40 km/h (11.1 m/s), except while driving inside the RI and CI, where the speed limit is 30 km/h (8.3 m/s) (Panis et al., 2011). These limits are well depicted in Figure 7, where inside intersections (gray areas) all vehicle speeds drop at least to 8.3 m/s, while outside intersections the vehicle speed may rise to 11.1 m/s. From Table 7, columns "*mean consumption*" it is possible to verify that the engine running on gasoline has a lower fuel consumption. This is due to the higher H_l value of gasoline. The TTW^{CO2} emissions (see columns "*mean TTW emission CO_2*") are approximately the same, registering a slight increase for the engine running on ethanol. The small difference in TTW^{CO2} regardless of the significantly different amount of fuel consumption, is due to the production of less CO_2 per ethanol molecule in the process of combustion. However, when considering the CO_2 emissions from all production chain of ethanol and gasoline WTW^{CO2} (see columns "*mean WTW emission CO_2*") emissions are no longer approximate. The WTW^{CO2} results show that ethanol has a higher well-to-wheel CO_2 emissions than gasoline, and consequently a higher environmental impact. The use of EMITM has a positive impact on the CO_2 emissions reduction. The reduction in CO_2 emissions, occurs for all traffic densities and is roughly 48.5%$. Detailed quantitative results can be observed in Table 7. The simulation results, also indicate, that more vehicles can go through the intersections with non or little stopping, when using any ITM as opposed to using standard traffic regulating techniques (see column "*time stopped*"). Since engines consume significant amounts of fuel and emit large amounts of gas pollution during slowing down to stop and speeding up to reach a free-flow speed again, the proposed algorithm EMITM, contributes to the fuel-efficient use, and emissions reduction. The consequence of non or little stopping is that the "mean speed" is similar to the "mean speed while in motion", see Figure 9.

In the results, we have assumed the presence of a ST-SP system on all vehicles. If this system was

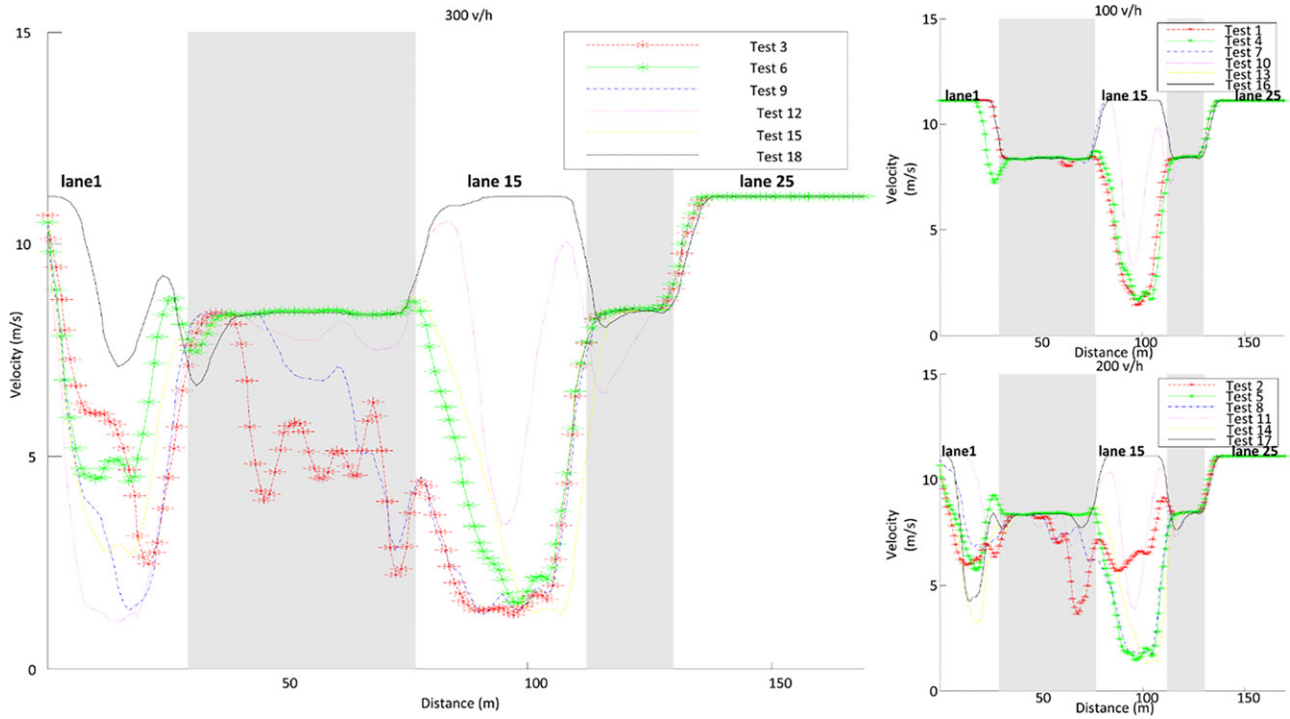

Figure 7. Mean speed profile vs. distance traveled of vehicles entering on lane 1 and exiting on lane 25 (the path between lane 1 and 25 passing through 15 is marked on Figure 6). The marked gray area at the distance traveled [30–70] and [110–130] represent the RI and CI, respectively. Mean speed profiles for both TFP1, TFP2, and TFP3 are on the left, center, and right subplots, respectively. The ITM used for Test *i*, where $i = \{1.18\}$, are presented in Table 7.

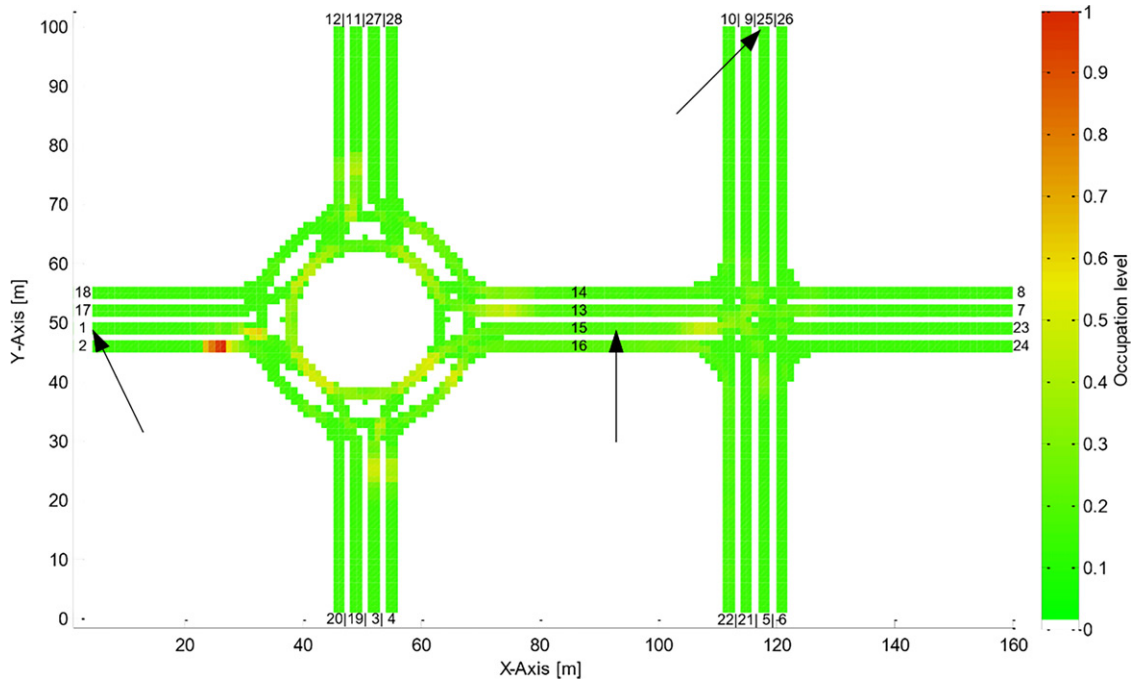

Figure 8. Simulation scenario layout (RI and CI) and cell occupancy level for simulation Test 18. Higher occupancy levels occur mainly on approaching and inside intersections. The path between lane 1 and 25 passing through lane 15 is used to study the vehicles speed profile in Figure 7.

considered to be unavailable, it would mean that part of the time the engine was idling, that is, the engine powering the vehicle was running when the vehicle was not moving. The effect of the absence of ST-SP system on the CO_2 emissions would be more noticeable in the simulation tests where the "*time stopped*" (see Table 7) is greater, which means that vehicles would spend more time on waiting, therefore, more time on engine idling and consequently more CO_2 emissions. Since the use of EMITM reduces the "*time stopped*", the absence of ST-SP system would mean a greater CO_2 emission reduction than the 48.5% presented above.

Table 8. Vehicle mechanical specifications.

Parameters		Value	
Vehicle mass	m_{veh}	1500	[kg]
Frontal area	A_f	2.0	[m^2]
Air drag coeffi.	C_D	0.3	[-]
Air density	ρ_{air}	1.2	[kg/m^3]
Rolling frict. coeffi.	C_R	0.01	[-]
Maximum boost ratio	Π_{max}	1	[m]
Gear ratios	γ	5(13.8, 7.7, 5.3, 3.9, 3)	[-]

Table 9. Otto cycle engine specifications.

Parameters		Value	
Displacement	V_d	1.5×10^{-3}	[m^3]
Bore	B	45×10^{-3}	[m]
Stroke	S	50×10^{-3}	[m]
Friction model	K_1	1.44×10^5	[Pa]
	K_2	0.46	[-]
	K_3	9.1×10^{-4}	[s^2/m^2]
	K_4	0.075	[m]
Gas exchange losses	ρ_{me0g}	1	[Pa]
Engine efficiency	ϵ	0.4	[-]
Gas exchange losses	$DFCO$	ON	[-]
Gear ratios	$ST-SP$	ON	[-]

Conclusions

Although a large IEEE 802.11 wireless communication system was simulated, the packet collision on this network did not prevent the ITM to fulfill its role. An extension to the previous CS was successfully introduced, that is, the SINR was used to measure the quality of the transmission channel.

A spatiotemporal reservation-based technique was proposed to reduce traffic congestion, vehicle fuel consumption, and CO_2 emission levels. For safety purposes, an extra area A_{safety} was reserved by the spatiotemporal reservation scheme. Although the ITM algorithms do not know the vehicles position, this safety area enables vehicles to cross the intersections without accidents. The spatiotemporal reservation scheme had a better performance than the traditional control scheme: lower intersection

Table 10. Fuel characteristics.

Gasoline				Ethanol			
Parameters		Value		Parameters		Value	
Density	$\rho_{C_8H_{18}}$	0.75	[kg/l]	Density	$\rho_{C_2H_5}$	0.75	[kg/l]
Lower eating value	$H_l^{C_8H_{18}}$	44.4	[MJ/kg]	Lower eating value	$H_l^{C_2H_5}$	44.4	[MJ/kg]
Molar mass	$M_{C_8H_{18}}$	114.22	[g/mol]	Molar mass	$M_{C_2H_5}$	114.22	[g/mol]
Well to tank	$WTT_{C_8H_{18}}^{CO_2}$	12.5	[gCO_2/MJ]	Well to tank	$WTT_{C_2H_5}^{CO_2}$	12.5	[gCO_2/MJ]
Carbon dioxide							
Parameters		Value					
Molar mass	M_{CO_2}	44.01	[g/mol]				

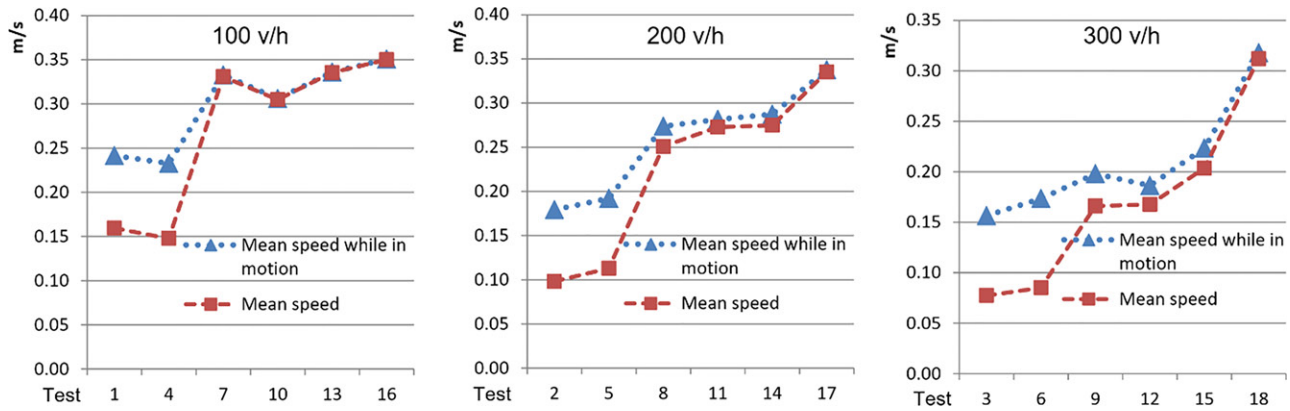

Figure 9. Mean speed while in motion and mean speed for each traffic flow when using EMITM algorithm.

traversing time, higher probability for non or little stopping, and less CO_2 emissions. The *Environmental Impact* module gave the ISR-TRAFSIM the ability to compute the fuel consumption and CO_2 emissions. The EMITM was demonstrated to be an efficient method for ITM producing improvements in traffic flow. Simulation results also suggested that the CO_2 emissions could be reduced more than 50% when using EMITM. The conversion of the simulator architecture to a socket-based multi-client intersection connected to a managing server is marked as future work, as well as the validation of both proposed algorithms and the ISR-TRAFSIM simulator.

Disclosure statement

No potential conflict of interest was reported by the authors.

Funding

This work was partially supported by the Portuguese Foundation for Science and Technology (FCT) and COMPETE under grant PTDC/SEN-TRA/099413/2008 (EVSIM09 Project) and UID/EEA/00048/2013. We also acknowledge the support of Project B-Mobility4People (QREN-MaisCentro SCT-2011-01) and the USA TranLIVE University Transportation Center.

ORCID

Luís Conde Bento https://orcid.org/0000-0002-9689-3637
Hesham A. Rakha https://orcid.org/0000-0002-5845-2929
Urbano J. Nunes https://orcid.org/0000-0002-7750-522

References

Alvarez, A. G., Martinez, P. J. P., & Franco, I. G. (2013). Energy consumption and carbon dioxide emissions in rail and road freight transport in Spain. *Journal of Intelligent Transportation Systems*, *17*(3), 233–244. DOI:10.1080/15472450.2012.719456

Bento, L. C., Parafita, R., & Nunes, U. (2012a). Inter-vehicle sensor fusion for accurate vehicle localization supported by V2V and V2I communications. In *IEEE International Conference on Intelligent Transportation Systems (ITSC)*, Anchorage, USA. https://doi.org/10.1109/itsc.2012.6338889

Bento, L. C., Parafita, R., & Nunes, U. (2012b). Intelligent traffic management at intersections supported by V2V and V2I communications. In *IEEE International Conference on Intelligent Transportation Systems (ITSC)*, Anchorage, USA. https://doi.org/10.1109/itsc.2012.6338766

Dresner, K., & Stone, P. (2008). A multiagent approach to autonomous intersection management. *Journal of Artificial Intelligence Research*, *31*, 591–656. https://doi.org/10.1613/jair.2502

Driel, C., & Arem, B. (2010). The impact of a congestion assistant on traffic flow efficiency and safety in congested traffic caused by a lane drop. *Journal of Intelligent Transportation Systems*, *14*(4), 197. https://doi.org/10.1080/15472450.2010.516226

Edwards, R., Larive, F., & Beziat, C. (2011). Well-to-wheels analysis of future automotive fuels and powertrains in the European Context WELL-to-WHEELS report. European Commission Joint Research Centre, Institute for Energy, version 3c.

Ferreira, M., & Orey, P. (2012). On the impact of virtual traffic lights on carbon emissions mitigation. *IEEE Transactions on Intelligent Transportation Systems*, *13*(1), 284–295. https://doi.org/10.1109/tits.2011.2169791

Guzzella, L., & Onder, C. (2004). *Introduction to modeling and control of internal combustion engine systems*. Berlin, Germany: Springer Verlag.

Guzzella, L., & Sciarretta, A. (2005). *Vehicle propulsion systems: Introduction to modeling and optimization*. Berlin, Germany: Springer Verlag.

Johnson, K. (2008). A plug-in hybrid electric vehicle loss model to compare wellto-wheel energy use from multiple sources (MSc Thesis). Virginia Pol Inst and State University, Blacksburg, VA.

Koonce, P., Rodegerdts, L., Lee, K., Quayle, S., Beaird, S., Braud, C., & Urbanik, T. (2008). Traffic signal timing manual, No: FHWA-HOP-08-024.

Liimatainen, H. (2011). Utilization of fuel consumption data in an ecodriving incentive system for heavy-duty vehicle drivers. *IEEE Trans on Intelligent Transportation Systems*. *12*(4), 1087–1095. https://doi.org/10.1109/tits.2011.2142182

Mendes, A., Bento, L. C., & Nunes, U. (2004). Multi-target detection and tracking with a laser scanner. In *IEEE Intelligent Vehicles Symposium*. Parma, Italy. https://doi.org/10.1109/IVS.2004.1336486

Milakis, D., Arem, B., & Wee, B. (2017). Policy and society related implications of automated driving: A review of literature and directions for future research. *Journal of Intelligent Transportation Systems*, *21*(4), 324–348. https://doi.org/10.1080/15472450.2017.1291351

Minjie, Z., Xu, L., Hongyu, H., Linghe, K., & Minglu, L. (2009). LICP: A look-ahead intersection control policy with intelligent vehicles. In *International Conference on Mobile Adhoc and Sensor Systems (MASS)*, Macau, China. https://doi.org/10.1109/mobhoc.2009.5336944

Munoz-Organero, M., & Magana, V. (2013). Validating the impact on reducing fuel consumption by using an ecodriving assistant based on traffic sign detection and optimal deceleration patterns. *IEEE Transactions on Intelligent Transportation Systems*, *14*(2), 1023–1028. https://doi.org/10.1109/tits.2013.2247400

Nunes, U., & Bento, L. C. (2007). Data fusion and path-following controllers comparison for autonomous vehicles. *Nonlinear Dynamics Journal*, *49*(4), 445–462. https://doi.org/10.1007/s11071-006-9108-y

Olia, A., Abdelgawad, H., Abdulhai, B., & Razavi, S. (2016). Assessing the potential impacts of connected vehicles: Mobility, environmental, and safety perspectives. *Journal*

of Intelligent Transportation Systems, *20*(3), 229. https://doi.org/10.1080/15472450.2015.1062728

Palomar, E., Fuentes, J., Gonzalez-Tablas, A., & Alcaide, A. (2012). Hindering false event dissemination in VANETs with proof-of-work mechanisms. *Transportation Research Part C: Emerging Technologies*, *23*, 85. https://doi.org/10.1016/j.trc.2011.08.002

Panis, L., Beckx, C., Broekx, S., Vlieger, I., Schrooten, L., Degraeuwe, B., & Pelkmans, L. (2011). PM, NO_x and CO_2 emission reductions from speed management policies in Europe. *Transport Policy*, *18*(1), 32–37. https://doi.org/10.1016/j.tranpol.2010.05.005

Park, S., Rakha, H., Farzaneh, M., Zietsman, J., & Lee, D. (2010). Development of fuel and emission models for high speed heavy duty trucks, light duty trucks, and light duty vehicles. In *IEEE International Conference on Intelligent Transportation Systems*, Funchal, Portugal. https://doi.org/10.1109/itsc.2010.5624972

Pinkerton, F., & Herbst, J. (2010). *Hydrogen-powered cars. McGraw-Hill Yearbook of Science and Technology*. New York, USA: McGraw-Hill.

Qiu, J., Guoyuan, W., Boriboonsomsin, K., & Barth, M. (2012). Advanced intersection management for connected vehicles using multi-agent systems approach. In *IEEE Intelligent Vehicles Symposium (IV)*, Alcala de Henares, Spain. https://doi.org/10.1109/ivs.2012.6232287

Ray, S., Carruthers, J., & Starobinski, D. (2005). Evaluation the masked node problem in AdHoc wireless LANs. *IEEE Transactions on Mobile Computing*, *4*(5), 430–442. https://doi.org/10.1109/tmc.2005.66

Safarianova, S., Noembrini, F., Boulouchos, K., & Dietrich, P. (2011). WP1 report: Techno-economic analysis of low-GHG emission passenger cars. In *Technology Opportunities and Strategies Toward Climate-Friendly Transport (TOSCA project)*. Project FP7-TRANSPORT ID 234217.

Shan, H., Sadek, A., & Yunjie, Z. (2012). Assessing the mobility and environmental benefits of reservation-based intelligent intersections using an integrated simulator. *IEEE Trans on Intelligent Transportation Systems*, *13*(3), 1201–1214. https://doi.org/10.1109/tits.2012.2186442

Sharma, S., & Mishra, S. (2013). ITS enabled optimal emission pricing models for reducing carbon footprints in a bi-modal network. *Journal of Intelligent Transportation Systems*, *17*(1), 54. https://doi.org/10.1080/15472450.2012.708618

Sommer, C., Krul, German, R. R., & Dressler, F. (2010). Emissions vs travel time: Simulative evaluation of the environmental impact of ITS. In *IEEE Vehicular Technology Conf (VTC 2010-Spring)*, Taipei, Taiwan. https://doi.org/10.1109/vetecs.2010.5493943

Suthaputchakun, C., Zhili, S., & Dianati, M. (2012). Applications of vehicular communications for reducing fuel consumption and CO_2 emission. *IEEE Communications Magazine*, https://doi.org/10.1109/mcom.2012.6384459

Wipke, K., Cuddy, M., & Burch, S. (1999). ADVISOR 21: a user-friendly advanced powertrain simulation using a combined backward/forward approach. *IEEE Transactions on Vehicular Technology*, *48*(6), 1751–1761. https://doi.org/10.1109/25.806767

Wojtowicz, J., & Wallace, W. (2010). Traffic management for planned special events using traffic microsimulation modeling and tabletop exercises. *Journal of Transportation Safety and Security*, *2*(2), 102. https://doi.org/10.1080/19439962.2010.487635

Yang, H., Wang, X., & Yin, Y. (2012). The impact of speed limits on traffic equilibrium and system performance in networks. *Transportation Research Part B: Methodological*, *46*(10), 1295–1307. https://doi.org/10.1016/j.trb.2012.08.002

Yao, E., & Yuanyuan, S. (2013). Study on eco-route planning algorithm and environmental impact assessment. *Journal of Intelligent Transportation Systems*, *17*(1), 42. https://doi.org/10.1080/15472450.2013.747822

Zhang, Y., Yang, L., & Ma, J. (2008). *Unlicensed mobile access technology: Protocols, architectures, security, standards and applications*. Florida, USA: CRC Press–Taylor and Francis Group.

Zhou, Y., Evans, G., Chowdhury, M., Wang, K., & Fries, R. (2011). Wireless communication alternatives for intelligent transportation systems: A case study. *Journal of Intelligent Transportation Systems*, *15*(3), 147. https://doi.org/10.1080/15472450.2011.594681

Zohdy, I., & Rakha, H. (2013). Enhancing roundabout operations via vehicle connectivity. *Transportation Research Record: Journal of the Transportation Research Board*, *2381*(1), 91. https://doi.org/10.3141/2381-11

Zohdy, I., & Rakha, H. (2016). Intersection management via vehicle connectivity: The intersection cooperative adaptive cruise control system concept. *Journal of Intelligent Transportation Systems*, *20*(1), 17. https://doi.org/10.1080/15472450.2014.889918